

2006

In-Situ Performance Evaluation of No-Frost Evaporators

Claudio Melo

Federal University of Santa Catarina

Robson O. Piucco

Federal University of Santa Catarina

Publio O. O. Durate

Whirlpool Corporation

Follow this and additional works at: <http://docs.lib.purdue.edu/iracc>

Melo, Claudio; Piucco, Robson O.; and Durate, Publio O. O., "In-Situ Performance Evaluation of No-Frost Evaporators" (2006).
International Refrigeration and Air Conditioning Conference. Paper 839.
<http://docs.lib.purdue.edu/iracc/839>

This document has been made available through Purdue e-Pubs, a service of the Purdue University Libraries. Please contact epubs@purdue.edu for additional information.

Complete proceedings may be acquired in print and on CD-ROM directly from the Ray W. Herrick Laboratories at <https://engineering.purdue.edu/Herrick/Events/orderlit.html>

IN-SITU PERFORMANCE EVALUATION OF NO-FROST EVAPORATORS

Cláudio MELO^{1,*}, Robson O. PIUCCO¹, Publio O. O. DUARTE²

¹Department of Mechanical Engineering, Federal University of Santa Catarina
P.O. Box 476, 88040-900, Florianópolis, SC, BRAZIL
Phone: +55 48 3234 5691, e.mail: melo@polo.ufsc.br, * Corresponding Author

²Multibrás Appliances S.A., Whirlpool Corporation
Rua Dona Francisca 7200, 89219-901, Joinville, SC, Brazil
Phone: +55 47 3441 4072, e.mail: Publio_O_Duarte@multibras.com.br

ABSTRACT

This paper outlines the thermal-hydraulic performance of no-frost evaporators in practical circumstances. A specifically designed experimental apparatus capable of controlling the air temperature around the refrigerator as well as the system operating conditions was extensively used during the tests. The air temperature was controlled by means of an environmental test room, constructed according to the specifications of the ISO 7371 (1985) standard. The system operation conditions were controlled by an experimental set-up based on a vapor compression refrigeration loop. Tests were carried out to explore the thermal-hydraulic performance of a particular no-frost evaporator with distinct flow arrangements (standard, counter-flow and parallel-flow). The results were all expressed in terms of the friction and Colburn factors, both as functions of the Reynolds number.

1. INTRODUCTION

The energy issue is one of the most serious environmental problems of modern times and it is directly related to the low efficiencies of the thermal systems currently in use. According to recent data of the National Program for Electric Power Conservation (Eletrobrás, 2000), the refrigeration sector represents approximately 11% of the total Brazilian electric power consumption. Despite their relative low energy consumption, household refrigerators represent a significant part of the national electric power consumption due to the large number of units in operation and also due to their low thermodynamic efficiencies.

In the Brazilian context, the most commonly sold refrigerators, and consequently those with the greatest impact on the national energy consumption, are those with two refrigerated compartments and with automatic defrost, commonly known as no-frost refrigerators. The main characteristic of a no-frost refrigerator is an air distribution system, comprised of a fan, damper, ducts and a tube-fin heat exchanger. The refrigerator air is forced across the evaporator by means of an axial fan located downstream of the heat exchanger. Cold and dehumidified air is supplied to a plenum, and from there part of it is directed to the freezer compartment (~70%) and part to the fresh-food compartment (~30%).

The air is supplied to the freezer compartment with speeds of the order of 2.0m/s and with temperatures around -30°C, for a room temperature of 32°C. After circulating in this compartment, the air returns to the evaporator through a return duct system whose openings are located in the freezer bottom side, close to the door. The airflow rates to the individual compartments are controlled by the action of a thermo-mechanical damper installed in a lateral duct at the back of the fresh-food compartment. The return air from the freezer and fresh-food compartments are mixed together at the inlet of the evaporator. The design and proper operation of the air distribution system strongly affect the refrigerator performance, in particular, the resulting temperature of the warmest package (ISO 8561, 1995).

The research effort reported herein has previously received attention from many researchers, although most of them have focused their attention on the evaporator only. Lee et al., (2002), for instance, compared the thermal performance of spine finned tube, continuous flat-plate fin-tube and discrete flat-plate fin-tube type no-frost evaporators, using an experimental apparatus constructed as an open wind tunnel. The heat transfer mechanism in

the evaporator was thermally reversed by circulating hot water from a thermostatic bath through the tubes. Janssen et al., (2000) carried out a similar study, also with a wind tunnel, but using a specifically designed refrigeration loop to control the evaporator operation conditions. Karatas et al., (2000) replaced the refrigerator air distribution system with two specifically designed wind tunnels, maintaining the evaporator, plenum and fan of the original system. The heat transfer mechanism in the evaporator was also reversed. A particular feature of this test set-up was the possibility to carry out tests with non-uniform air temperature and velocity fields at the evaporator inlet.

In this study the refrigerator itself was used as a test section maintaining unchanged all the geometric characteristics of the air distribution system. The refrigerator was placed within an environmental test room and connected to a refrigeration loop, located at the outside of the chamber and capable of controlling and measuring the system operation conditions. The set-up enables the investigation of the effect of several parameters, such as evaporation pressure, fan speed, refrigerant quality at the entrance of the evaporator, refrigerant mass flow rate, airflow rate, and number, shape and position of the air supply openings, on the refrigerator performance. The experimental apparatus can also be used to characterize the evaporator performance in terms of the friction factor f and Colburn j factor as functions of the Reynolds number, which was the object of this work.

2. EXPERIMENTAL APPARATUS

As mentioned above a two-door top-mount 430-liter no-frost refrigerator was used as a test section. The refrigerator was firstly placed in a test room, kept at 32°C and constructed according to the ISO 7371 (1985) standard. The refrigerator was then connected to a specifically designed refrigeration loop, also known as an evaporator calorimeter (see Figure 1), through which the system operation conditions were varied, controlled and measured (Melo et al., 2004).

The HFC-134a mass flow rate and the system pressures were controlled by a manual metering valve and by a variable speed compressor. The subcooling at the condenser outlet was regulated through the combined action of a thermostatic bath and a PID-controlled electric heater. The air temperatures at the internal and external sides of the refrigerator were measured by T-type thermocouples, embedded in copper cylinders and strategically distributed according to the ISO 7371 (1985) standard, with an uncertainty of $\pm 0.2^\circ\text{C}$. The air inlet and outlet temperatures across the sample coils were obtained from the arithmetic means of the readings of eight T-type thermocouples, all embedded in copper cylinders, half installed downstream and half upstream of the heat exchanger. The air temperature and relative humidity measurement stations are illustrated in Figure 2.

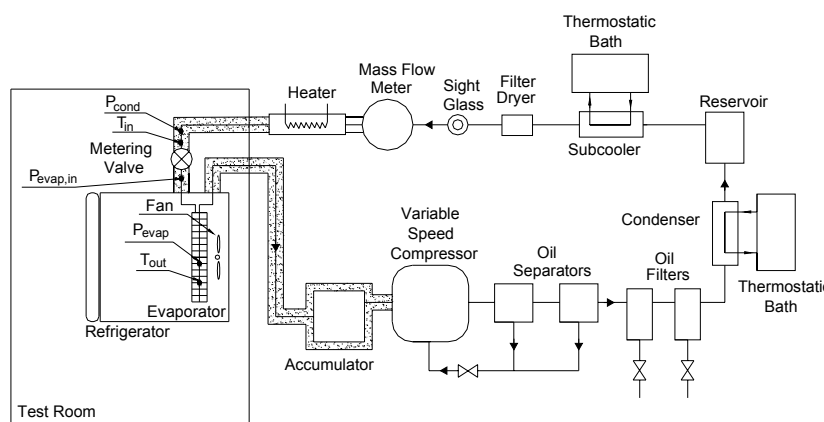


Figure 1: Schematic diagram of the refrigeration loop

The refrigerant pressure and temperature at the outlet of the evaporator were monitored by absolute pressure transducers with an uncertainty of $\pm 0.01\text{bar}$, and by T-type immersion thermocouples with an uncertainty of $\pm 0.2^\circ\text{C}$, respectively. The evaporator air pressure drop was detected by a differential pressure transducer, with a measurement range of 50 Pa, and with a maximum error of ± 0.25 Pa. Plastic hoses with micro holes were used as pressure taps and installed upstream and downstream of the evaporator (Figure 3a). The opening of the thermo-mechanical damper was also controlled by a specifically designed device, as shown in Figure 3b. The output signals from the transducers and thermocouples were collected and converted by a computerized data acquisition system.

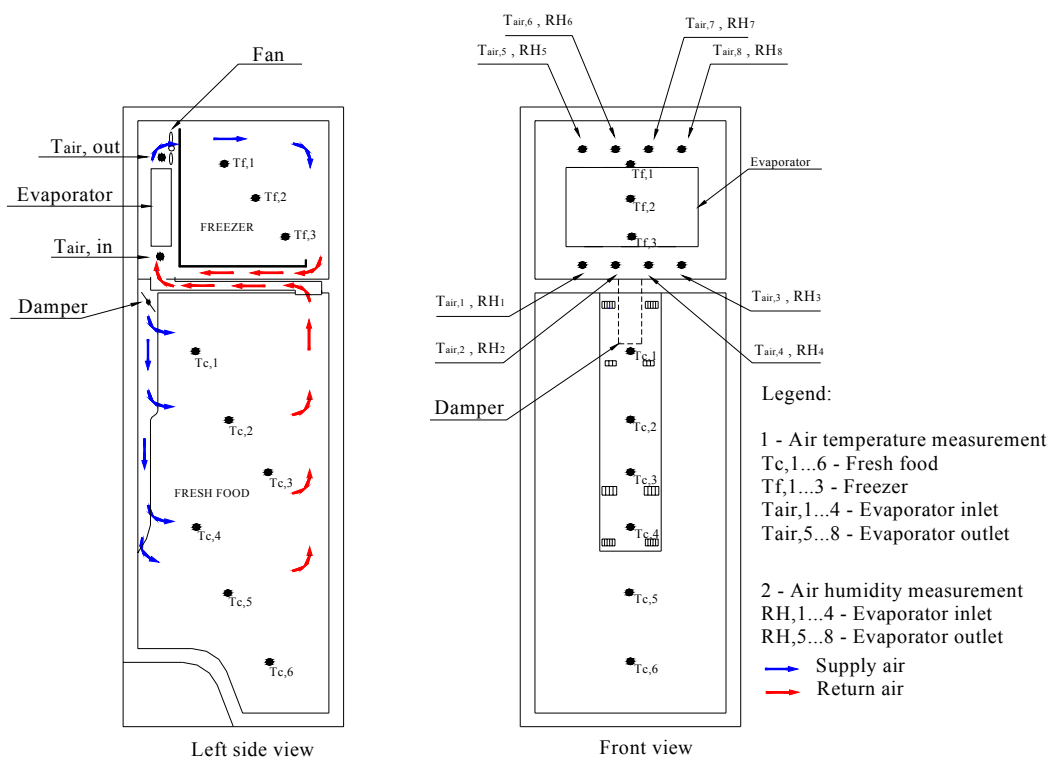


Figure 2: Temperature and relative humidity measurement stations

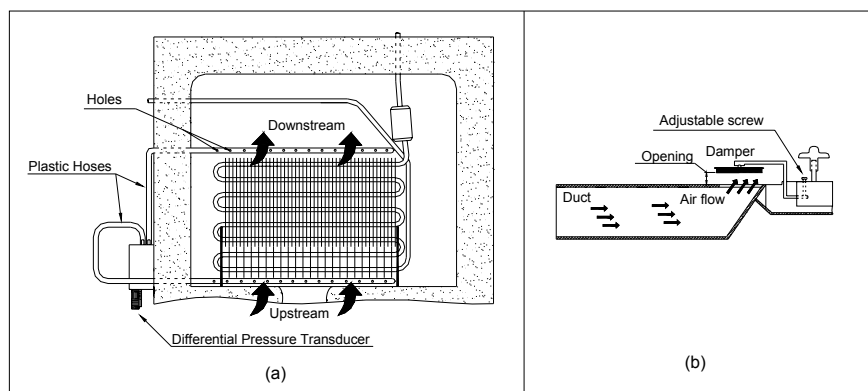


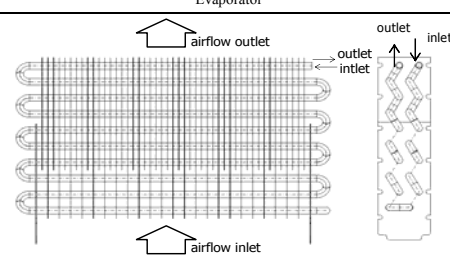
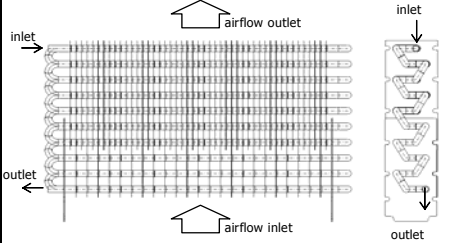
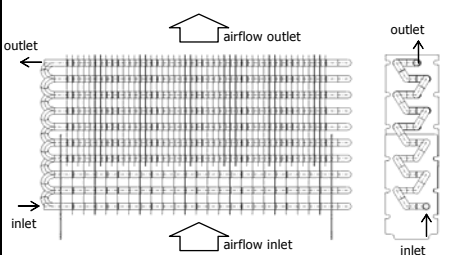
Figure 3: (a) Evaporator air pressure drop measurement; (b) Damper opening control

3. EXPERIMENTAL PROCEDURE AND RESULTS

The refrigerator was firstly placed in a test room, kept at 32°C. As soon as steady-state conditions were reached the evaporator calorimeter was switched-on. The adjustment of a particular test condition required, on average, 60 minutes. The test set-up was maintained for at least 30 minutes at the test condition, before recording any data. The experimental data were then recorded for a period of 15 minutes. A 5-minute period, with the lowest level of scattering, was then extracted from the 15-minute period, over which the averaged values were calculated.

As mentioned above the experimental apparatus introduced in the previous section was used to assess the thermal-hydraulic performance of a particular no-frost evaporator, with three different flow arrangements. Their detailed geometric parameters are tabulated in Table 1.

Table 1: Geometric characteristics of the evaporators

Evaporator	Characteristics
	Type: Standard Tube Diameter, m: 0.00794 Tubes per row: 2 Number of fins: 24 (large) Number of fins: 23 (short) Face Area, m ² : 0.02083 Minimum Flow Area, m ² : 0.01485 Finning Factor: 5.263
	Type: Counter-Flow Tube Diameter, m: 0.00794 Tubes per row: 2 Number of fins: 24 (large) Number of fins: 23 (short) Face Area, m ² : 0.02083 Minimum Flow Area, m ² : 0.01485 Finning Factor: 5.212
	Type: Parallel-Flow Tube Diameter, m: 0.00794 Tubes per row: 2 Number of fins: 24 (large) Number of fins: 23 (short) Face Area, m ² : 0.02083 Minimum Flow Area, m ² : 0.01485 Finning Factor: 5.212

The evaporators were tested varying the fan speed, the damper opening, the refrigerant quality at the inlet of the evaporator and the evaporation pressure in a random way and using the values listed in Table 2. The system cooling capacity (\dot{Q}_e) was determined from an energy balance in the refrigerant side, expressed as follows:

$$\dot{Q}_e = \dot{m}_r (h_{r,o} - h_{r,i}) \quad (1)$$

where \dot{m}_r , $h_{r,o}$ and $h_{r,i}$, correspond to the refrigerant mass flow rate and the refrigerant enthalpy at the outlet and inlet of the evaporator, respectively.

The evaporator superheat (ΔT_e) was calculated from the difference between the refrigerant temperature at the outlet of the evaporator ($T_{r,o}$) and the evaporation temperature (T_{sat}), as follows:

$$\Delta T_e = T_{r,o} - T_{sat} \quad (2)$$

Table 2: Test conditions

Fan Speed [rpm]	Damper Opening [mm]	Quality [%]	Evap. Pressure [bar]
2235	without damper	33	0.885 (-29°C)
2565	1.2	38	0.731 (-33°C)
2745	2.5	42	0.662 (-35°C)
2895	6.5		
3060			
3165			

In steady-state conditions the evaporator superheat is usually very small, and therefore most of the tests in this study were conducted at a null superheat condition (evaporator completely filled with refrigerant). However, low

superheat measurements are very difficult to be made since, at that range, some liquid droplets are still dispersed in the superheated vapor refrigerant flow.

On the other hand, it was found that the cooling capacity varied in a linear and inverse way with the evaporator superheat (see Figure 4a), and that the air temperature and relative humidity at the inlet and outlet of the evaporator were almost constant for superheat values lower than 5°C (see Figure 4b).

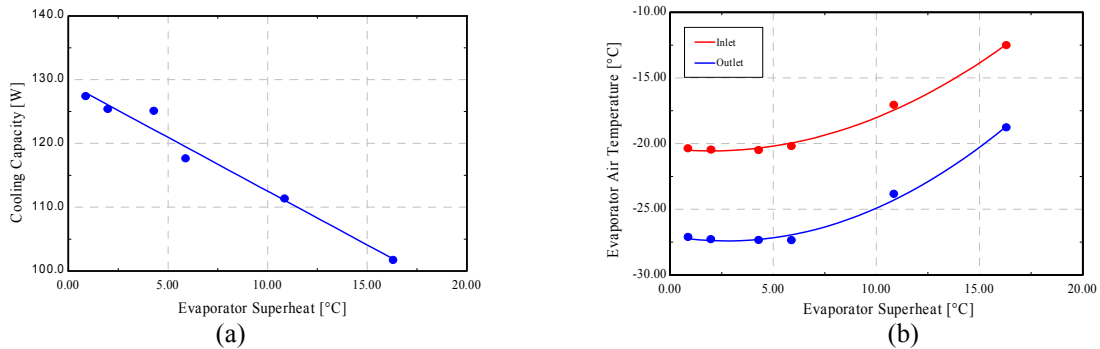


Figure 4: (a) Cooling capacity and (b) evaporator inlet and outlet air temperatures as functions of superheat

To avoid the low superheat measurements, three tests were then carried out for each test condition specified in Table 2. The refrigerant mass flow rate was varied between the tests, keeping all other variables constant. In this way three distinct evaporator superheats were obtained for the same test condition, all higher than 2°C. The cooling capacity and the inlet and outlet air temperatures and relative humidity were then obtained by linear extrapolation, as shown in Figures 5, 6a and 6b (Melo et al., 2005).

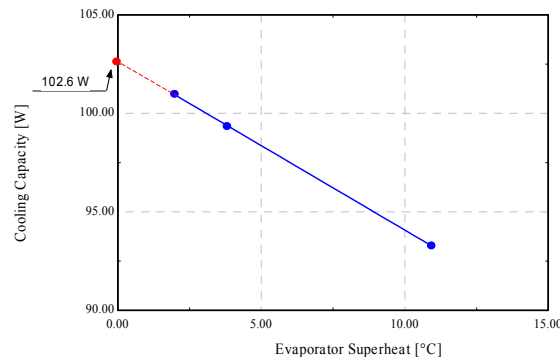


Figure 5 – Cooling capacity versus superheat

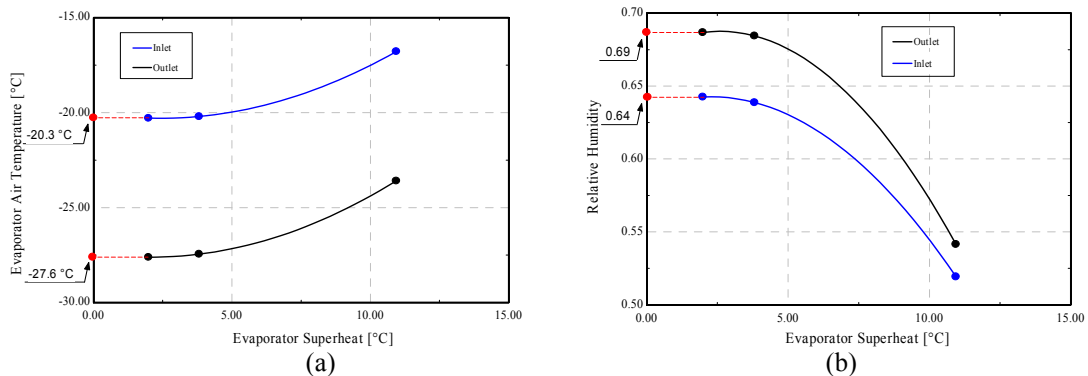


Figure 6: Air properties versus superheat: (a) temperature and (b) relative humidity

The heat transfer characteristics of each evaporator were expressed in terms of the Colburn j factor, as follows:

$$j = \frac{Nu}{Re \cdot Pr^{1/3}} = a \cdot Re^{b-l} \quad (3)$$

where the Nusselt and Reynolds numbers, are given as follows:

$$Nu = h_a D / k_a \quad (4)$$

$$Re = G_{max} D / \mu_a \quad (5)$$

where k , μ , D , G_{max} and h_a symbolize the air thermal conductivity, the air absolute viscosity, the evaporator tube outer diameter, the refrigerant mass flux at minimum flow area and the air side convective heat transfer coefficient, respectively. All the fluid properties were evaluated at the average values of the inlet and outlet air temperatures under steady state condition.

The air-side heat transfer coefficient was calculated as follows:

$$h_a = \left\{ \left(\frac{A_o}{UA} \right) - \left[\frac{A_o}{A_i} \right] \frac{1}{h_{r,i}} \right\}^{-1} \quad (6)$$

where A_o and A_i stand for the external and internal surface area of the evaporator tubes, respectively. The tube-side heat transfer coefficient ($h_{r,i}$) was evaluated from the Dittus-Boelter equation. The overall thermal conductance (UA) of the evaporator was obtained as follows:

$$UA = \frac{\dot{Q}_e}{\frac{(T_{a,i} - T_{sat}) - (T_{a,o} - T_{sat})}{\ln \frac{(T_{a,i} - T_{sat})}{(T_{a,o} - T_{sat})}}} \quad (7)$$

where $T_{a,i}$ and $T_{a,o}$ are the inlet and outlet evaporator air temperatures, respectively.

The evaporator air pressure drop was expressed by a friction factor, f , as follows:

$$\Delta p = \frac{G_{max}^2}{2\rho_i} \left[\left(1 + \sigma^2 \right) \left(\frac{\rho_i}{\rho_o} - 1 \right) + f \frac{A_o}{A_{min}} \frac{\rho_i}{\rho_m} \right] \quad (8)$$

where A_{min} , ΔP and σ represent the minimum flow area, the evaporator air pressure drop and the ratio of minimum flow area to face area of the coil, respectively. The sub-indexes i , o and m represent the evaporator inlet, outlet and average condition, respectively.

Figure 7a shows the Colburn j factor as a function of the Reynolds number for the standard evaporator. A similar relationship is shown in Figure 7b, but including the counter-flow and parallel-flow evaporators. As expected, at a null superheat condition, the evaporator thermal performance did not vary as a function of the flow arrangement, and can be generically expressed as:

$$j = 0.098 \text{Re}^{-0.312} \tag{9}$$

Also, the evaporator performance did vary as a function of the Reynolds number (damper opening and fan speed) only, being unaffected by the evaporation pressure and refrigerant quality (see Table 2).

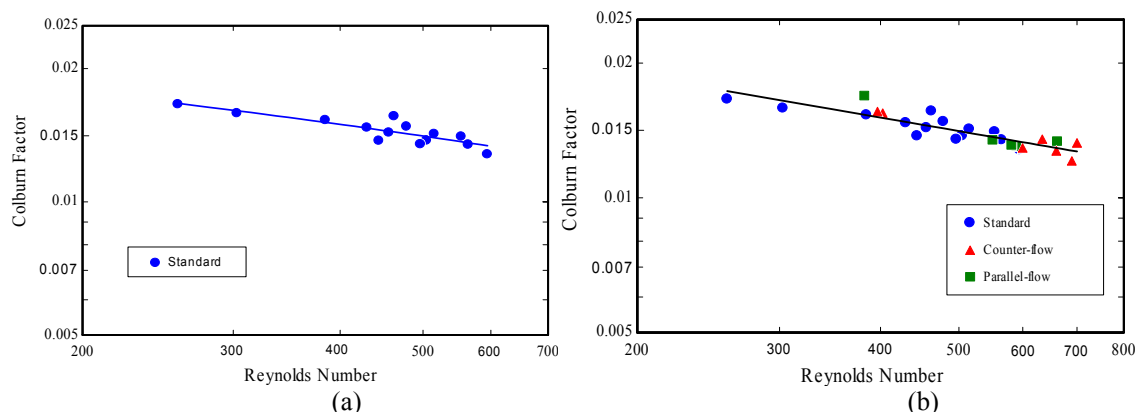


Figure 7: Colburn j factor versus Reynolds number (superheat=0)

Figure 8a illustrates the relationship between the Colburn j factor and the Reynolds number for the three evaporators under study and for an evaporator superheat of 5°C. It can be observed that there was no difference in the evaporator performance, probably because most of the superheat occurred in the suction line and not in the evaporator tubes. A similar comparison is shown in Figure 8b, but for a superheat of 10°C. At that condition it was found that the thermal performance of the counter-flow evaporator was 45% higher than that of the original evaporator. This may be important, particularly during the transient regimes of operation when the evaporator superheat is quite high.

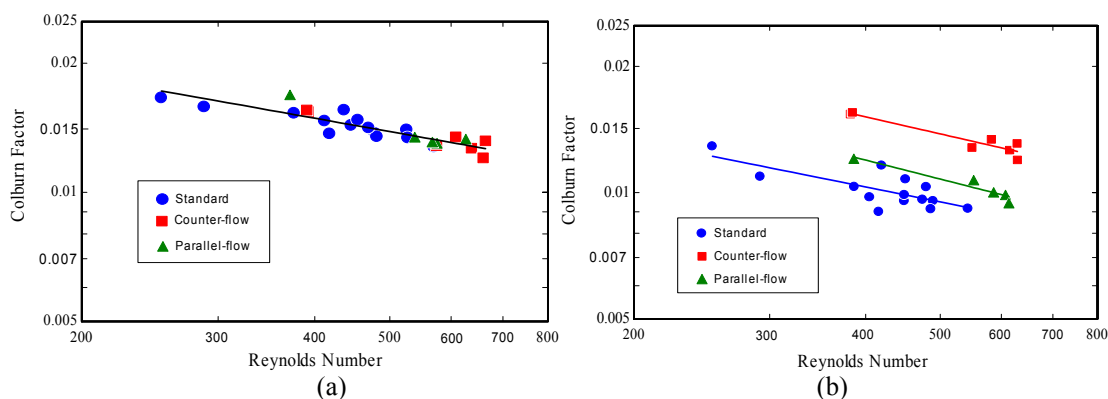


Figure 8: Colburn factor versus Reynolds number: (a) (superheat=5°C); (b) (superheat=10°C)

The standard evaporator air pressure drop is illustrated in Figure 9a and expressed mathematically in equation (10), as a relationship between the friction factor, f , and the Reynolds number, as follows:

$$f = 234.95 \text{Re}^{-1.14} \tag{10}$$

Figure 9b illustrates the first-order j/f performance evaluation criteria for the heat exchanger under study at a null superheat condition. It can be seen that the evaporator performance increases with the Reynolds number, indicating that the growth of the evaporator heat transfer rate exceeds that of the evaporator pressure drop as the Reynolds number increases.

4. CONCLUSIONS

An experimental apparatus capable of evaluating the thermal-hydraulic behavior of no-frost evaporators in practical circumstances was developed. This means that the evaporators were tested in the way in which they are installed into a household refrigerator, using the same air distribution system and the original refrigerant.

Three evaporators of similar design, but with distinct flow arrangements (standard, parallel-flow and counter-flow) were tested varying the fan speed, the refrigerant quality at the inlet of the evaporator, the evaporation pressure and the damper opening. It was found that the evaporator performance was only affected by the damper opening and fan speed. It was also found that the evaporator performance was unaffected by the flow arrangement at superheat values lower than 5°C. The counter-flow heat exchanger offered a higher heat transfer performance, at a 10°C superheat condition, than the other heat exchangers considered in this study.

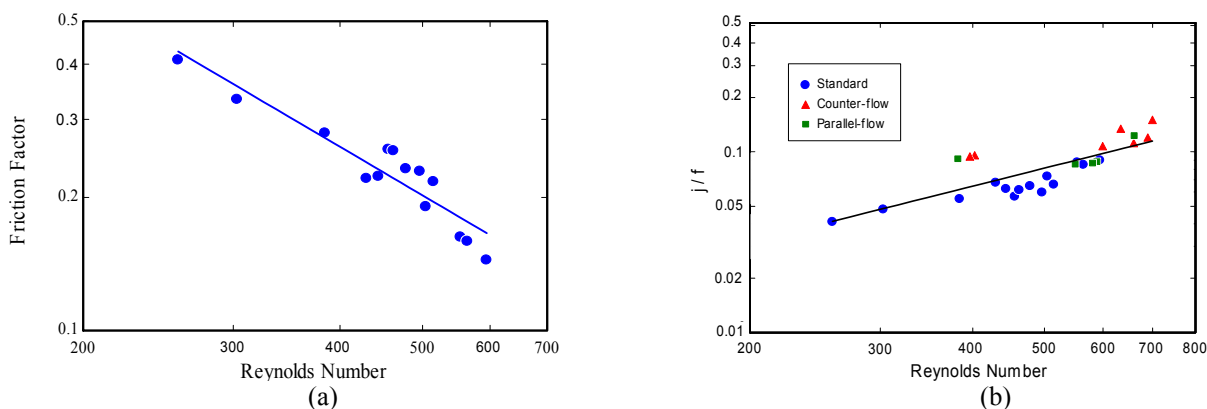


Figure 9: (a) Friction factor versus Reynolds number and (b) j/f performance evaluation criteria

REFERENCES

- Eletrobrás, 2000, PROCEL: National Program of Electrical Energy Conservation, <http://www.eletrobrás.gov.br/procel>.
- ISO 8561, 1995, Household Frost-Free Refrigerating Appliances – Refrigerators, Refrigerator-Freezers, Frozen Food Storage Cabinets and Food Freezers Cooled by Internal Forced Air Circulation – Characteristics and Test Methods.
- ISO 7371, 1985, Performance of Household Refrigerating Appliances – Refrigerators With or Without Low Temperature Compartment.
- Karatas, H., Dirik, E., Derbentli, T., 2000, An Experimental Study of Air-side Heat Transfer and Friction Factor Correlations on Domestic Refrigerator Finned-Tube Evaporator Coils, Eighth International Refrigeration and Air Conditioning Conference at Purdue, West Lafayette, Indiana – USA, July 25-28.
- Janssen, M. Wijnstekers, J., Becks, P., Kuijpers, L., In-Situ Evaporator Heat Transfer Experiments for Domestic Refrigerators, Eighth International Refrigeration and Air Conditioning Conference at Purdue, West Lafayette, Indiana – USA, July 25-28.
- Lee, T-H., Lee, J-S, Oh, S-Y, Lee, M-Y, 2002, Comparison of Air Side Heat Transfer Coefficients of Several Types of Evaporators of Household Freezer/Refrigerators, Ninth International Refrigeration and Air Conditioning Conference at Purdue, West Lafayette, Indiana – USA, July 16-19.
- Melo, C., Pottker, G., Waltrich, M., Piucco, R. O, 2004, Calorimeter for the Thermal-Hydraulic Evaluation of No-Frost Evaporators, Internal Research Report, Federal University of Santa Catarina, Florianópolis, SC, Brazil (in Portuguese).
- Melo, C., Piucco, R. O., Boeng, J., 2005, Thermal-Hydraulic Performance of No-frost Evaporators, Part IV, Internal Research Report, Federal University of Santa Catarina, Florianópolis, SC, Brazil (in Portuguese).

ACKNOWLEDGEMENTS

The authors are grateful to Multibrás Eletrodomésticos S.A. for sponsoring this research program and for technical discussions, in particular, Mr Marco E. Marques. Thanks are also due to Messrs Gustavo Pottker, Maicon Waltrich and Joel Boeng for their dedicated work during the construction of the test setup.